SERS FROM PYRIDINE ADSORBED ON ELECTRODISPERSED PLATINUM ELECTRODES ☆

S.A. BILMES [1], J.C. RUBIM [2], A. OTTO
Physikalisches Institüt III. Universität Düsseldorf, D-4000 Düsseldorf, Federal Republic of Germany

and

A.J. ARVIA
INIFTA, Universidad de La Plata, Suc. 4, CC 16, 1900 La Plata, Argentina

Received 17 February 1989; in final form 18 April 1989

SERS of pyridine adsorbed on electrodispersed platinum electrodes is reported. Electrodispersed platinum surfaces are obtained by electroreducing hydrous platinum oxide layers. The intensity of the Raman scattering for adsorbed pyridine is enhanced by at least one order of magnitude, after normalizing with respect to the area increase. The estimated Raman enhancement factor is lower than that reported for roughened silver electrodes but it is still sufficiently large to allow Raman scattering from adsorbates on platinum to be detectable. Surface changes (ageing) of the metal surface can be also followed by SERS.

1. Introduction

Surface-enhanced Raman scattering (SERS) has been extensively used in the study of Ag, Cu and Au surfaces covered with a large number of adsorbates [1]. In either electrochemical environments or in air or under UHV conditions the increase in the Raman scattering is always related to the morphology of the substrate. As a general rule some degree of surface roughness is required to observe SERS although the actual influence of surface roughness on the scattering process is not yet completely understood. On the other hand, metal surfaces with high catalytic activity, i.e. Pt, Pd or Rh, have not as yet shown SERS comparable to that observed on Ag, Au and Cu. The Raman spectrum of phenylhydrazine adsorbed on platinum electrodes was obtained when the electrode was activated until the surface looked "yellowish gray" [2] but this result could not be reproduced [3]. Raman scattering of CO adsorbed on slightly platinized platinum electrodes [4] and on roughened Au electrodes covered by electrodeposited platinum [5] has also been observed. Small but significant SERS was found for Py adsorbed on colloidal Pt [6] and sputtered platinum films [7] as well as for benzene adsorbed on small Pt clusters [8]. In the course of the application of Fourier transform near infrared spectroscopy on Raman scattering from electrode surfaces [9] a good signal from pyridine on platinum was obtained [10]. Recently, unenhanced Raman scattering from 4-cyanopyridine adsorbed on polycrystalline Rh electrodes has been reported [11]. This technique seems to be promising for the determination of surface configurations of adsorbates in electrochemical systems.

Electrodynamic calculations of the surface-enhanced electromagnetic intensity at the surface of platinum spheroids in air and in water showed that the enhancement increases and its maximum shifts to longer wavelengths as the spheroid size increases from 10 to about 100 nm [12]. At the tip of a spheroid with semimajor axis of 101 nm in air, the ab-

☆ Dedicated to the memory of Professor Haruka Yamada.

[1] Present address: Departamento de Química Inorgánica, Analítica y Química Física, Facultad de Ciencias Exactas y Naturales, Universidad de Buenos Aires, Ciudad Universitaria, Pab II, 1428 Buenos Aires, Argentina.

[2] Alexander von Humboldt Stiftung Fellow. Permanent address: Instituto da Quimica da USP, CP 20780, 01478 Sao Paulo, SP, Brazil.

0 009-2614/89/$ 03.50

solute maximum of 76.2 is reached at 710 nm incident radiation [12], whereas in water the corresponding values are 74.3 at 960 nm.

A very effective procedure to achieve an electrodispersed platinum surface with a roughness factor ranging from 2 to 10^3 is the two-stage method recently described in the literature [13,14]. First a square wave between an upper (≈ 2.0 V_{SCE}) and a lower (≈ -0.3 V_{SCE}) potential is applied to the Pt specimen in acid aqueous electrolyte at frequencies of the order of a few kHz for 2 to 60 min to accumulate a hydrous platinum oxide layer. This is electroreduced in the second stage at a constant potential ($E \leqslant 0$ V_{SCE}) or by a potential sweep from the upper limit of the square wave to ≈ -0.3 V_{SCE} at sweep rates $v \leqslant 10$ mV/s. The resulting rough platinum overlayer (electrodispersed) was studied by ex situ scanning electron microscopy and scanning tunneling microscopy [15]. It can be modelled as a large number of spheroids of ≈ 10 nm diameter. These surfaces also exhibit interesting electrocatalytic properties [16].

This communication reports the Raman spectra of pyridine (Py) adsorbed on electrodispersed platinum electrodes under different ageing conditions. Even though Py is adsorbed on platinum electrodes over the whole range of stability of water [17] this adsorbate was chosen in order to compare its Raman enhancement factor on this type of Pt surface with those estimated from the Raman spectra of pyridine adsorbed on other SERS active substrates.

2. Experiment

Raman spectra were obtained using a SPEX 1404 double monochromator equipped with holographic gratings (2400 grooves/mm). A RCA (C 31034-02) photomultiplier was used as detector. The exciting wavelength was the 514.5 nm line from an Ar^+ laser with an operating power of ≈ 150 mW measured near the spectroelectrochemical cell. The angle of incidence was about 45° and the electric vector of the incident beam was in the plane of incidence (p-polarization). To avoid local heating effects two orthogonal cylindrical lenses were employed to focus the laser line on the electrode surface. The Raman scattered light was collected within a cone normal to the surface without polarization discrimination [18]. All spectra were obtained with a spectral slit width of 5 cm^{-1} at 0.1 Å s^{-1}.

Experiments were carried out in a conventional electrochemical cell. The working electrodes were circular platinum foils (0.7 cm diameter, 2 mm thickness. Johnson–Matthey spectroscopically pure) in contact with a copper rod for electrical contact. They were embedded in PTFE to ensure that only the platinum surface was exposed to the electrolyte. They were polished with Al_2O_3 papers down to 1 μm particle size and then rinsed with doubly distilled water. The potential of the working electrode was measured with respect to a saturated calomel electrode. A large platinum wire was used as counterelectrode.

The electrodispersed platinum electrodes were obtained in the following way. First a polished platinum electrode was cycled at 0.1 V/s in 1 M H_2SO_4 between -0.24 and 1.2 V (versus SCE) in order to check the surface cleanliness conditions and to determine the effective area by the H-adatom electroadsorption charge [19]. Then the working electrode was subjected to a repetitive square wave potential between -0.24 and 2.2 V with a half period ranging from 0.2 to 1 ms pulse width during ≈ 5–15 min to accumulate a relatively thick hydrous platinum oxide layer. Subsequently, the potential was held at -0.24 V until the complete electroreduction of the hydrous platinum oxide layer was accomplished. As the active surface area of these electrodes decreases by about 20% on continuous potential cycling at 0.1 V/s in the potential range of water stability, two types of roughened platinum electrodes were employed, namely freshly prepared electrodes and aged electrodes, i.e. stabilized by repetitive potential cycling at 0.1 V/s between -0.24 and 1.2 V at room temperature. The freshly prepared electrodes were only subjected to a few ($\leqslant 10$) triangular potential cycles at 0.1 V/s between -0.24 and 0.2 V. Finally the electrode was carefully rinsed with water and immediately transferred to the working cell containing deaerated 0.1 M Na_2SO_4 and 0.04 M Py. After the spectrochemical experiments the electrode was reimmersed in the cell containing 1 M H_2SO_4 and cycled at 0.1 V/s between -0.24 and 1.2 V. This last step was done to check variations in the electroadsorption charge of the H adatoms.

The large geometrical area of the electrodes used in the spectroelectrochemical cell caused a non-uniform potential and current distribution at the surface during the roughening treatment. Consequently both fresh and aged roughened platinum electrodes exhibit patches with different visual appearence ranging from gray to brownish. Aged and freshly prepared roughened platinum electrodes can be easily distinguished by the color of the central surface region as the latter appears bright yellow or brownish for the freshly prepared electrodes but slightly greyish for the aged electrodes. The real area of the electrode was measured by the H-adatom monolayer electroadsorption charge in 1 M H_2SO_4. The roughness factor R of the electrodispersed platinum electrodes was obtained from the ratio between the real and geometric area. Thus, R is a parameter averaged over the entire electrode area whereas the laser radiation is focused on a smaller region.

All reagents were analytical grade and doubly distilled water was employed for the preparation of solutions.

3. Results

The Raman spectra of smooth and electrodispersed platinum electrodes immersed in 0.1 M Na_2SO_4 and 0.04 M pyridine aqueous solution at $E=0$ V are shown in fig. 1. The smooth electrode (fig. 1a) presents a strong Raman signal at 982 cm^{-1} from the stretching mode of SO_4^{2-} in water, a moderate signal at 1003 cm^{-1} due to the symmetrical breathing mode of pyridine in water and a weaker one at 1035 cm^{-1} assigned to the trigonal breathing mode of pyridine in water. The Raman spectrum in fig. 1a originates from the solution layer close to the electrode surface. The Raman spectrum of an electrodispersed, fresh platinum electrode with a value of $R=65$ clearly displays a broad and asymmetric Raman band between 1010 and 1020 cm^{-1} (fig. 1b). Its intensity exceeds that of the band at 982 cm^{-1} from the solution. The bands of pyridine in solution at 1003 and 1036 cm^{-1} appear as shoulders of the band at 1016 cm^{-1}. For the aged electrode (fig. 1c) the band at 1016 cm^{-1} has a relatively low intensity and is not clearly discriminated from the solution spectrum. The Raman spectra resulting for both types

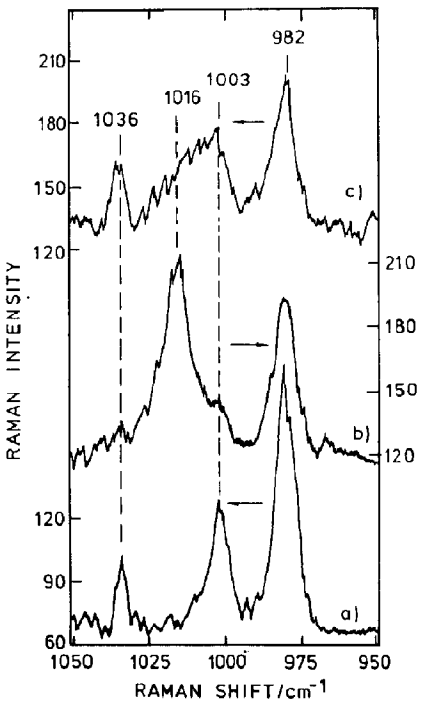

Fig. 1. Raman spectra obtained by using different platinum electrodes immersed in 0.1 M Na_2SO_4+0.04 M pyridine, at 0 V (versus SCE). $\lambda=514.5$ nm, $P=120$ mW (at the cell). (a) Smooth Pt electrode ($R=1.8$); (b) electrodispersed (fresh) Pt electrode ($R=65$); (c) aged electrodispersed Pt electrode ($R=36$).

of electrodispersed platinum electrodes in the absence of Py exhibit only the signal corresponding to the SO_4^{2-} stretching mode at 982 cm^{-1} over the entire potential range covered by the present work. The difference in the intensity of the Raman bands attributed to the species in the solution layer (i.e. 982, 1003 and 1035 cm^{-1}) for electrodispersed and smooth electrodes is tentatively explained by differences of optical reflectivity. Only a small increase in the background ($\approx$60 cps) is observed for an electrodispersed platinum electrode as compared to smooth platinum. The integrated intensity of the Raman signal in the 1010–1020 cm^{-1} region was measured for electrodispersed (fresh) platinum electrodes with values of R ranging from 19 to 269. The results exhibit no correlation between the value of R and the integrated intensity I of the Raman band at 1014 cm^{-1} normalized to the integrated intensity of

the band at 1003 cm^{-1} (see table 1, first four rows). This is a first indication that the Raman enhancement is due to the size and shape of metal clusters and not to the extent of the real surface area. The maximum intensity for this band has been obtained for freshly prepared electrodispersed platinum electrodes when the focus area shows an intense yellow colour. For aged electrodispersed platinum electrodes, the intensity of the band at ≈ 1013 cm^{-1} reaches a maximum when the incident beam is focused on the brownish regions of the surface.

Fig. 2 shows the Raman spectrum of Py adsorbed at -0.2 V on an electrodispersed platinum electrode with $R = 150$, covering different spectral regions. In this case clear Raman signals are observed at 643, 1014, 1212 and 1599 cm^{-1}. The intensity of the ≈ 1014 cm^{-1} band for adsorbed pyridine is reduced to $\approx 80\%$ after holding the potential for 30 min at -0.1 V.

Table 1
I is the integrated intensity of the 1014 cm^{-1} band relative to that of the 1003 cm^{-1} band for different samples of fresh electrodispersed Pt electrodes at $E = -0.2$ V. R is the roughness factor obtained by hydrogen electroadsorption (see text). G is the value of the enhancement of the Raman enhancement, normalized by the roughness factor, under the assumption of a 1:1 pyridine to Pt surface coverage (see text)

Sample No.	R	I	I/R	G
1	19	2.3	0.121	55
2	55	3.1	0.056	65
3	71	4.1	0.057	
4	101	1.1	0.011	6
5	141	0	0.021	
6	150	3.1	0.021	
7	200	3.5	0.018	
8	269	2.1	0.008	

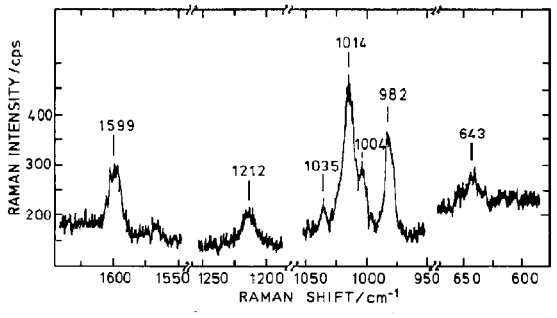

Fig. 2. Raman spectrum of pyridine adsorbed on a electrodispersed (fresh) platinum electrode ($R = 150$) at -0.2 V. $\lambda = 514.5$ nm, $P = 180$ mW (at the cell). Bands of pyridine in water are at 617, 1003, 1217 and 1576 cm^{-1} (see table 2).

The intensity and position of the Raman signal depicted in fig. 1b depends on the applied potential E (see fig. 3). As the potential increases, the Raman signal is shifted to higher wavenumbers (fig. 3a). The direction of this shift is the same as for the symmetrical breathing mode of pyridine adsorbed on SERS-active silver electrodes [20] but the gradient of the shift versus E is larger in our case (see fig. 3b). The maximum intensity of the 1010–1020 cm^{-1} signal is obtained when E is set to the -0.2 to 0.2 V range. The intensity change of this band was followed by the potential–time program shown in fig. 3d; some representative spectra are depicted in fig. 3e. The spectra recorded at potentials $E \leqslant -0.3$ V exhibit a decrease (curve 2); the initial intensity at -0.1 V (curve 1) is not recovered at the same potential after an incursion into the $E \leqslant -0.3$ V region (curve 3). For $E \geqslant 0.3$ V the intensity of this band also decreases as is evident for curve 4. In the potential range (-0.43 to 0.65 V) the I/E profile recorded between two successive potentiostatic runs is close to the cyclic voltammogram (full line in fig. 3c). The band at 1010–1020 cm^{-1} is completely suppressed after a few minutes at $E = 0.78$ V (curve 5). In this case the potential scan from 0.78 to -0.1 V shows an increase in the cathodic current (dashed line in fig. 3c) related to the electroreduction of an oxygen-containing layer on platinum. The Raman spectra recorded at -0.1 V after the potential sweep from 0.78 V shows that the intensity of the ≈ 1015 cm^{-1} band is almost completely recovered (curve 6). The voltammograms obtained in 1 M H_2SO_4 after the spectrochemical experiments in the Py-containing solutions show a decrease in the current related to the H and O electroadsorption processes. This indicates that Py is adsorbed on Pt over the entire potential range. This conclusion coincides with that of Lane and Hubbard [17] with polycrystalline platinum and favours in principle the proposed idea that Py can also be adsorbed on PtO [21]. In this sense, the present results show a quenching of the Raman intensity in the potential range where O-containing

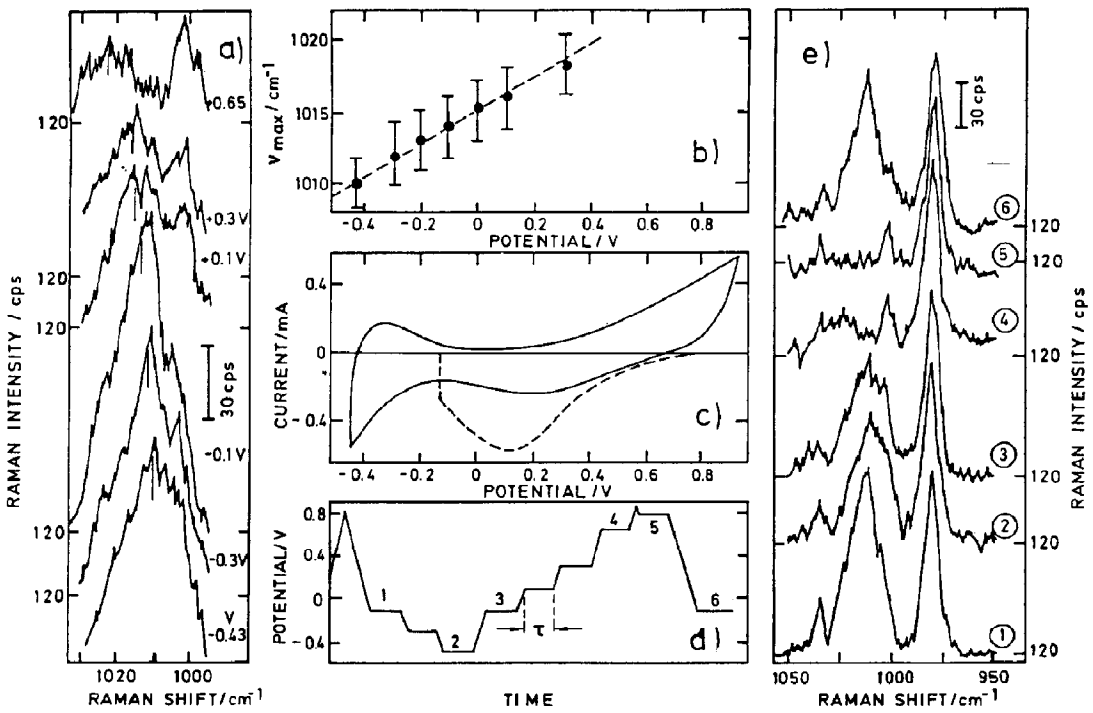

Fig. 3. (a) Raman band at 1010–1020 cm^{-1} as a function of the potential. (b) Position of the band in (a) versus potential. (c) Full line: voltammogram of a freshly electrodispersed platinum electrode in 0.1 M Na_2SO_4 + 0.04 M pyridine electrolyte (sweep rate = 50 mV s^{-1}). Dashed line: after keeping the potential at 0.78 V for 20 min (see text). (d) Potential–time program corresponding to the Raman spectra of (e); $15 \leqslant \tau \leqslant 20$ min; sweep rate = 50 mV s^{-1}. (e) Raman spectra of the electrode at the potentials indicated in (d). Spectra and voltammogram were taken for a fresh electrodispersed Pt electrode ($R = 71$) under the same conditions as in fig. 1.

surface species can be electroformed on platinum, i.e. for $E > 0.65$ V.

4. Discussion

IR and Raman spectra of solid $[Pt(Py)_2Cl_2]$ and $[Pt(Py)_4]^{2+}$ (dissolved in water) complexes exhibit a shift in the symmetrical breathing mode of pyridine from 991 cm^{-1} [22] up to 1025 cm^{-1} [23,24]. On the other hand, high-resolution electron energy loss spectroscopy (HREELS) of Py adsorbed on Pt(111) [25] and on Pt(110) reveals the existence of a band in the 1010–1050 cm^{-1} range whose position depends on the temperature and surface crystallography. It has been assigned to the ring breathing of adsorbed pyridine. On this basis, the Raman signal observed in the 1010–1020 cm^{-1} range for electrodispersed platinum electrodes immersed in a pyridine-containing solution (fig. 1) whose position is potential dependent and which is not observed when smooth Pt electrodes are employed can be assigned to the breathing mode of pyridine adsorbed on platinum. Table 2 shows a comparison of the vibrational data for pure pyridine, pyridine aqueous solutions, Pt–Py complexes, pyridine adsorbed on platinum in UHV and pyridine adsorbed on electrodispersed platinum electrodes. It can be seen from fig. 2 and table 2 that the Raman signals at 643, 1014, 1212 and 1599 cm^{-1} found for electrodispersed platinum electrodes at −0.2 V (fig. 2) are also shifted with respect to those found in the Raman spectra of either pure Py or 0.04 M Py aqueous solution. The relative intensities of the bands in the HREEL spectra of Py adsorbed on Pt single crystals [25,27] and that shown in fig. 2 differ considerably

Table 2
Comparison of some vibrational frequencies of pyridine in systems involving Pt–Py interactions [a]

Sym. [b]	Mode [c]	Description	Py liquid [d]	Py/ H_2O [d]	Py/ H_2O [e]	$[Pt(Py)_2Cl_2]_{trans}$ [f]	Py/Pt(111) [g]		Py/ Pt(110) [h]	Py/ Pt(−0.2 V) [e]
							320 K	120 K		
A_1	8a	ring stretching	1582	1593	1595	1609	1570	1610	(1500)	1599
	19a	ring stretching	1483	1488	1489	–	1450	1470	1415	–
	9a	in-plane CH bend	1217	1217	1217	1218	1230	1230	1230	1212
	18a	in-plane CH bend	1069	1069	1070	1079				–
	12	assym. ring breathing	1030	1033	1035					
	1	sym. ring breathing	991	1001	1003	1023	1010	1050	1035	1014
	6a	in-plane ring deform.	604	616	617	647				642
B_2	8b	ring stretching	1574	1576	1576	1565	1570	1610		1599
	19b	ring stretching	1437	1441	–	–	1450	1470	1415	–
	3	in-plane CC bend	1227	1231	1234		1230	1230	1230	1212
	15	in-plane CH bend	1146	1150	1152	1151	1150			–
	6b	in-plane ring deform.	654	653	652	647	740	660		642

[a] Some bands are assigned to more than one mode due to uncertainty in the assignment.
[b] Notation as recommended in the report on notation for the spectra of polyatomic molecules [26].
[c] Wilson mode number for benzene. [d] Ref. [21]. [e] This work. [f] Ref. [23]. [g] Ref. [24]. [h] Ref. [25].

as one should expect for different selection rules involved in surface Raman scattering and in EELS. The Raman frequency assigned to the breathing mode of adsorbed Py as well as its shift to higher wavenumbers as the applied potential is increased, indicate that adsorbed Py is bonded to Pt surface atoms through the lone pair of electrons localized on the nitrogen atom, i.e. through a σ–donor interaction, which implies a "non-flat" adsorption. For an adsorption geometry with the ring plane oriented parallel to the surface (i.e. a π interaction) greater shifts should be expected for this vibrational mode as has been reported, for instance, for benzene adsorbed on different substrates [28]. Our conclusion of a "non-flat" adsorption configuration is in agreement with both HREELS [25,27] and near-edge X-ray absorption fine structure results for Py adsorbed on Pt(111) at 298 K [29]. Therefore, despite the environmental differences, a good correlation is found between Py adsorbed on platinum in the electrochemical system and in gas phase experiments.

The fact that the Raman band intensity at ≈1014 cm^{-1} is not simply correlated with the roughness factor R indicates that some kind of surface enhancement might be involved.

The enhancement factor was estimated from the ratio of the integrated band intensity of the symmetrical breathing mode obtained for adsorbed Py and for Py in aqueous solution in the scattering configurations in fig. 4. In the former case (fig. 4b) the plane of incidence was parallel to the direction W, the incident radiation was p-polarized. In the latter case (fig. 4a) the polarization of the laser beam was also parallel to the direction W. The Raman scattered light was not analyzed with respect to polarization. In these scattering configurations one does not need to know the focal depth of the imaging of

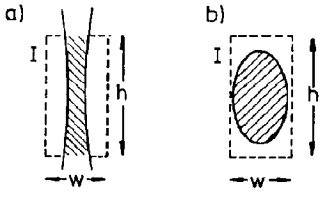

Fig. 4. Scattering configurations (a) for Raman scattering from solutions, (b) for Raman scattering from electrodes. I, image of the spectrometer slit on the sample; W, width; h, height.

the sample onto the spectrometer slit nor the waist diameter of the focused laser beam, provided it is smaller than the width W of the viewing field given by the image of the spectrometer entrance slit at the sample.

For a solution of Py, the integrated band intensity, I_v, can be expressed as

$$I_v = k_v N_v V_v \sigma_v I_v^0 = k_v N_v h \sigma_v P , \quad (1)$$

where k_v contains the physical constants and the experimental factor; N_v is the number of pyridine molecules per cm^3; V_v is the scattering volume which is determined by the product of the beam cross section Q_v and the height of the image of the spectrometer slit h ($h=2$ cm$/M$, M being the magnification of the collection lenses); σ_v is the effective Raman scattering cross section and I_v^0 is the intensity of the excitation beam ($I_v^0 = P/Q_v$, P being the power of the incident beam).

In the same way, for adsorbed Py

$$I_s = k_s N_s A_s \sigma_s I_s^0 = k_s N_s \sigma_s P , \quad (2)$$

where k_s is defined as k_v but for the configuration in fig. 4b; N_s is the number of adsorbed pyridine molecules per cm^2; A_s is the area of the laser beam focused by the cylindrical lenses onto the surface, which is assumed to be fully covered by the image of the spectrometer entrance slit. $I_s^0 = P/A_s$ is the intensity of the incident beam and σ_s is the effective Raman scattering cross section for the adsorbed Py. In the latter, both local electromagnetic field enhancement and "chemical effects" are included.

N_s can be estimated by assuming that the surface can adsorb as many pyridine molecules as hydrogen adatoms,

$$N_s = (q_H^0/e) R , \quad (3)$$

where q_H^0 is the electroadsorption charge of a monolayer of H adatoms on polycrystalline platinum, i.e. 0.22 mC cm^{-2} [19] and e the electron charge.

Assuming that the experimental factor is the same in both configurations depicted in fig. 4 (i.e. $k_v = k_s$), the estimated enhancement G is

$$G = \sigma_s/\sigma_v = I_s N_v P_v h / I_v N_s P_s , \quad (4)$$

where P_v and P_s are the power of the incident beam employed for the experiment with the aqueous solution and with the electrochemical cell. For the sake of comparison, both experiments were carried out one after the other to avoid any variation in the detector response.

Values of G for the pyridine breathing mode are quoted in the last row of table 1. They represent a minimum enhancement factor as a 1:1 Py:Pt ratio was assumed in eq. (3). From an comparison of the voltammetric charge corresponding to H-adatom electroadsorption run for the same Pt electrode in 1 M H_2SO_4 before and after the addition of Py up to 0.04 M, we determine a 1:3 Py:Pt ratio. This would increase the values of G in table 1 by a factor of 3.

The procedure described above to obtain G was only performed for samples 1, 2 and 4, yielding an average enhancement (on top of the area enhancement!) of about 40 (or 120 for a Py:Pt ratio of 1:3). Since the relative intensity I is a relative measure of the enhancement (remember that it involves a comparison of the intensities of Raman bands of adsorbed pyridine and pyridine in solution), and since the average value of I from samples 3, 5, 6, 7 and 8 of 2.56 is somewhat larger than the corresponding value of 2.16 for samples 1, 2 and 4, the quoted value of 40 appears representative.

In addition, successive Raman spectra performed in 0.1 M Na_2SO_4 + 0.04 M Py with an electrodispersed platinum electrode ($R=200$; $E=-0.2$ V) and a silver electrode activated by ORC up to 49 mC cm^{-2} ($E=-0.5$ V) indicate that the ratio between the integrated intensity for the breathing mode of pyridine adsorbed on Ag and on Pt is 300. That means that the enhancement factor on platinum is 2–3 orders of magnitude lower than that for silver under comparable conditions. Unfortunately, quantitative evaluations of the enhancement factor for pyridine adsorbed on silver electrodes are very sparse, ranging from 1.5×10^4 to 7×10^6 [30].

Our enhancement value is an average over all adsorbed pyridine molecules whereas the theoretical predictions of the intensity enhancement at the surface are only valid for molecules adsorbed at the tips of optimized spheroids [12]. This and the difficulties of averaging the local field factors for incident and emitted light over a statistical rough surface makes a quantitative comparison with the classical electromagnetic enhancement model impossible. The potential dependence of the Raman intensities in fig. 3 and the observed irreversibilities might indicate a

non-classical contribution to the observed enhancement.

5. Conclusions

SERS of pyridine adsorbed on electrodispersed platinum electrodes is reported for the first time. The preparation of electrodispersed platinum surfaces by electroreducing hydrous platinum oxide layers is a promising method of obtaining platinum surfaces for SERS of adsorbates on that metal. The breathing mode for adsorbed pyridine is found in the 1010–1020 cm^{-1} range indicating bonding via the nitrogen lone pair. The corresponding true enhancement factor is about one to two orders of magnitude. Although the estimated enhancement is lower than that reported for roughened silver surfaces [30], it is still sufficiently large to allow Raman scattering from adsorbates on catalytic metals like platinum. The extension of this method to other metals and adsorbates is currently in progress.

Acknowledgement

SAB is recipient of a post-doctoral fellow of the Consejo Nacional de Investigaciones Científicas y Técnicas (CONICET) from Argentina. JCR acknowledges the Alexander-von-Humboldt-Stiftung for the grant of a fellowship. SAB thanks I. Mrozek for many valuable discussions and experimental help.

References

[1] R.K. Chang, Ber. Bunsenges. Physik. Chem. 91 (1987) 296; A. Otto, in: Light scattering in solids, Vol. 4, eds. M. Cardona and G. Guntherodt (Springer, Berlin, 1983); M. Moskovits, Rev. Mod. Phys. 57 (1985) 783.
[2] J. Heitbaum, Z. Physik. Chem. NF 105 (1977) 307.
[3] J. Heitbaum, private communication.
[4] R.P. Cooney, M. Fleischmann and P.J. Hendra, J. Chem. Soc. Chem. Commun. (1977) 235.
[5] L.W.H. Leung and M.J. Weaver, J. Am. Chem. Soc. 109 (1987) 5113.
[6] R.E. Benner, K.U. Von Raben, K.C. Lee, J.F. Owen, R.K. Chang and B.L. Laube, Chem. Phys. Letters 96 (1983) 65.
[7] H. Yamada and Y. Yamamoto, Chem. Phys. Letters 77 (1981) 520.
[8] W. Krasser and A.J. Renouprez, Solid State Commun. 41 (1982) 231.
[9] A. Crookell, M. Fleischmann, M. Hanniet and R.J. Hendra, Chem. Phys. Letters 149 (1988) 123.
[10] M. Fleischmann, private communication.
[11] C. Shannon and A. Campion, J. Phys. Chem. 92 (1988) 1385.
[12] M.P. Cline, P.W. Barber and R.K. Chang, J. Opt. Soc. Am. B 3 (1986) 15.
[13] A.J. Arvía, J.C. Canullo, E. Custidiano, P.L. Perdriel and W.E. Triaca, Electrochim. Acta 146 (1983) 93.
[14] A.C. Chialvo, W.E. Triaca and A.J. Arvía, J. Electroanal. Chem. 146 (1983) 93.
[15] L. Vázquez, J. Gómez, A.M. Baró, N. García, M.L. Marcos, J. González, J.M. Vara and A.J. Arvía, J. Am. Chem. Soc. 109 (1987) 1730.
[16] M. Marcos, J.M. Vara, M. González Velasco and A.J. Arvía, J. Electroanal. Chem. 224 (1987) 189.
[17] R.F. Lane and A.T. Hubbard, J. Phys. Chem. 81 (1977) 734.
[18] J. Dünnwald, Dissertation, Universität Düsseldorf (1987).
[19] T. Biegler, D.A.J. Rand and R. Woods, J. Electroanal. Chem. 29 (1971) 269.
[20] A.B. Anderson, R. Kötz and E. Yeager, Chem. Phys. Letters 82 (1981) 130.
[21] E.A. Nechaev, T.F. Silina, V.A. Pavlichenko and E.V. Misnik, Soviet Electrochem. 22 (1986) 1289.
[22] H.D. Stidhamm and D.P. DiLella, J. Raman Spectry. 8 (1979) 180.
[23] F. Herbelin, J.D. Herbelin, J.P. Mathieu and H. Poulet, Spectrochim. Acta 22 (1966) 1515; J.R. Durig, B.R. Mitchele, D.W. Sink and J.N. Willis, Spectrochim. Acta 23A (1967) 1121.
[24] S.A. Bilmes and J.C. Rubim, in preparation.
[25] V.H. Grassian and E.L. Muetterties, J. Phys. Chem. 90 (1986) 5900.
[26] J. Chem. Phys. 23 (1955) 1997.
[27] M. Surman, S.R. Bare, P. Hofmann and D.A. King, Surface Sci. 179 (1987) 243.
[28] B.E. Koel, J.E. Crowel, G.M. Mate and G.A. Somorjai, J. Phys. Chem. 88 (1984) 1988.
[29] A.L. Johnson and E.L. Muetterties, J. Am. Chem. Soc. 105 (1983) 7183.
[30] M.J. Weaver, S. Farquarson and M.A. Tadayyoni, J. Chem. Phys. 82 (1985) 4867; M.G. Albrecht and J.A. Creighton, J. Am. Chem. Soc. 99 (1977) 5215.